IEEE OCEANS'95 Proceedings, October 1995

Effects of Air/Sea Conditions on Azimuth Modulations in K_u-Band Ocean Radar Backscatter

S. V. Nghiem, F. K. Li, and G. Neumann

Jet Propulsion Laboratory
California Institute of Technology
Pasadena, California 91109

Address: Dr. S. V. Nghiem, JPL MS 300-235, Tel: 818-354-2982
E-Mail: nghiem@Malibu.jpl.nasa.gov

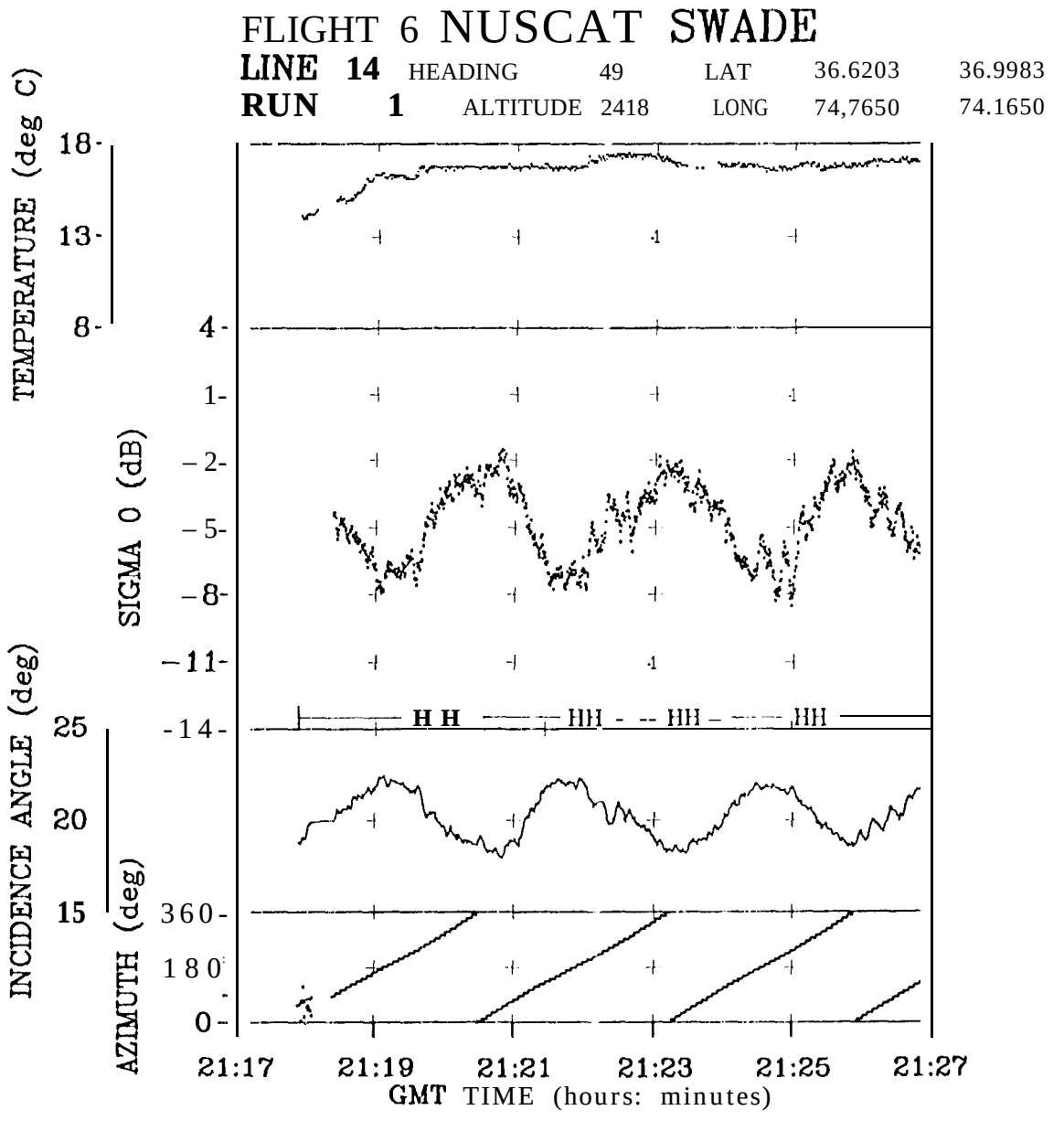

Figure 1. NUSCAT data sample including backscatter, incidence and azimuth angles

tudes up to 10000 m. The estimated relative calibration accuracy is ±0.23 dB and absolute error is about ±1 dB [5].

The NUSCAT/SWADE flights were carried out in 1991 off the coast of Maryland and Virginia. In the experimental area, several buoys were deployed: Discus C, Discus E, Discus N, CERC, and the National Oceanographic and Atmospheric Administration's Experimental buoy, or Coastal Buoy '2. Among data collected by buoys were wind speeds, wind directions, air and sea temperatures, significant wave heights, and directional wave spectra.

There was a total of 10 flights during 2/2/91-3/9/91 . The flights were partitioned into flight lines, and each line into runs. Flight lines included straight, triangle and radiator patterns. The NUSCAT data set consists of HH and VV backscattering coefficients, incidence and azimuth angles, time tags, latitudes and longitudes, and other ancillary data from aircraft such as altitude, pitch, roll and heading angles. A sample of the NUSCAT data is shown in Figure 1.

AZIMUTH MODULATIONS

Azimuth Signatures:

Azimuth modulations in ocean radar backscatter have two main features: the directional alignment effect in the wind direction and the asymmetry in the upwind and downwind directions. These effects can be described by a second harmonic function [7] which is specified by three different coefficients. In this paper, the azimuth modulations arc studied in terms of backscatter in the up, down, and crosswind directions, which determine the three coefficients. In this case, the harmonic function is expressed in the linear domain (not dB) as

$$\sigma_{PP} = \frac{1}{4}(\sigma_{PP}^{(u)} + \sigma_{PP}^{(d)} + 2\sigma_{PP}^{(c)}) + \frac{1}{2}(\sigma_{PP}^{(u)} - \sigma_{PP}^{(d)})\cos\phi + \frac{1}{4}(\sigma_{PP}^{(u)} + \sigma_{PP}^{(d)} - 2\sigma_{PP}^{(c)})\cos(2\phi)$$

where σ_{PP} is the backscattering coefficient at azimuth angle ϕ with respect to the wind direction. The backscatter in the upwind direction is $\sigma_{PP}^{(u)} = \sigma_{PP}(\phi = 00)$, downwind backscatter is $\sigma_{PP}^{(d)} = \sigma_{PP}(\phi = 180°)$, and crosswind backscatter is $\sigma_{PP}^{(c)} = \sigma_{PP}(\phi = 90°) = \sigma_{PP}(\phi = 270°)$ for polarization PP which can be horizontal HH or vertical VV.

Algorithm:

We need to extract from NUSCAT data the values of $\sigma_{PP}^{(u)}, \sigma_{PP}^{(d)}$, ancl $\sigma_{PP}^{(c)}$ to determine the azimuth modulations. Figure 1 Snows that there is a modulation in incidence angles that depend on azimuth angles. This was caused during the NUSCAT flights by a pitch angle resulting in a tilt of the antenna axis with respect to nadir. Note that circle flights may have similar problem caused by wind effects. This incidence modulation beats with the azimuth modulations in the ocean backscatter to create extraneous harmonics in the measured signals. We developed a method to account for the effects of incidence angle fluctuations and the extraneous harmonics in the retrieval of $\sigma_{PP}^{(u)}, \sigma_{PP}^{(d)}$, and $\sigma_{PP}^{(c)}$ using full azimuth scans of NUSCAT data. The algorithm does not involve any assumption on the underlying geophysical model functions and thus independent of such models. We carried out an end-to-end simulation to assess the performance of the algorithm. For 10°-600 incidence angles and all azimuth angles relative to wind direction, the simulation for horizontal polarization presented in Figure 2 indicates excellent results with small residual deviations (root-mean-square values within 0.15-0.25 dB). Vertical polarization results show similar performance. The simulation was also verified for all wind conditions of interest for SWADE.

Results:

We apply the above algorithm to NUSCAT/SWADE data to determine azimuth modulations in ocean backscattcr at various atmospheric and oceanic conditions measured by buoys. NUSCAT data are correlated with buoy measurements at the closest time and location. Upwind, downwind, and crosswind backscattering coefficients for horizontal polarization at 10°-60° incidence angles are shown in Figure 3 as functions of neutral wind speed U_N at 1 9.5-m height. The range of wind speed under consideration is from 4 m/s to 15 m/s. NUSCAT/SWADE results represented by the symbols ai e compared with RADSCAT results [1](continuous curves) and predictions from SASS-I [7] (dashed curves) and SASS-II [8] (clashed-dotted curves). It is known that there arc some discrepancies among RADSCAT, SASS-I, and SASS-II, which are seen in Figure 3. in general, NUSCAT/SWADE data are higher than RADSCAT results especially at larger incidence angles. At 10° incidence angles, NUSCAT/SWADE data fit best with SASS-1 and also compared well with SASS-II. At 20°300 incidence angles, NUSCAT, SASS-1, and SASS-II arc in good agreement and RADSCAT results are low. At larger incidence angles, NUSCAT data compare best with SASS-II. Results for vertical polarization have a best overall comparison with SASS-II.

SUMMARY

Ku-band backscatter data acquired by the Jet Propulsion laboratory airborne NUSCAT scatterometer during SWADE were analyzed

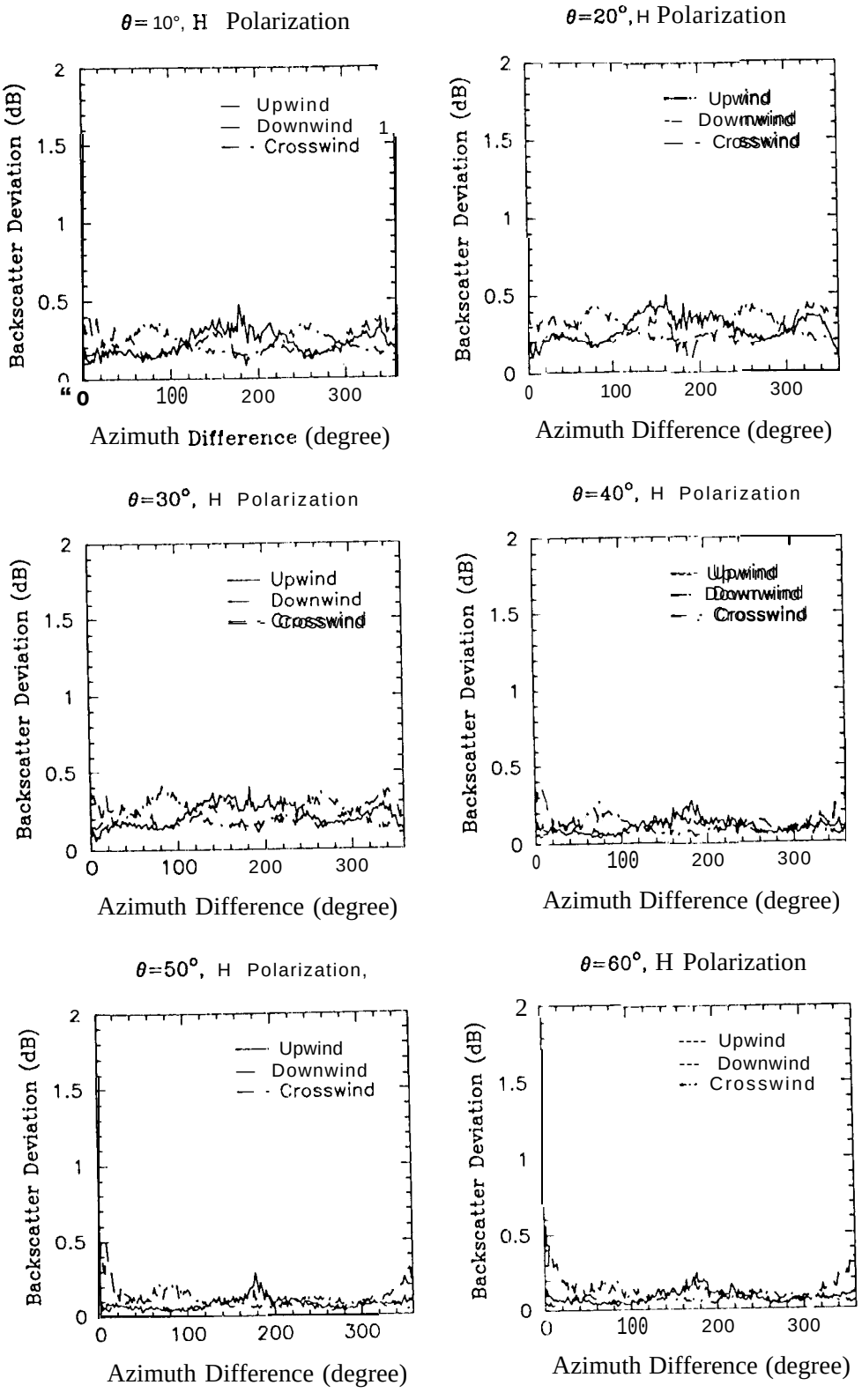

Figure 2. Simulation for performance assessment of the algorithm to determine azimuth modulations in NUSCAT/SWADE data. The vertical axis is for deviations from true values and the horizontal axis is for azimuth angles relative to the wind direction. This simulation is for horizontal polarization and incidence angles from 10° to 60°.

Figure 3. Backscattering coefficients at upwind, downwind, and crosswind for horizontal polarization as functions of neutral wind at 19..5 height. The symbols are for NUSCAT/SWADE data, continuous curves for RADSCAT results, dashed curves for SASS-I, and dash-dotted curves for SASS-II.

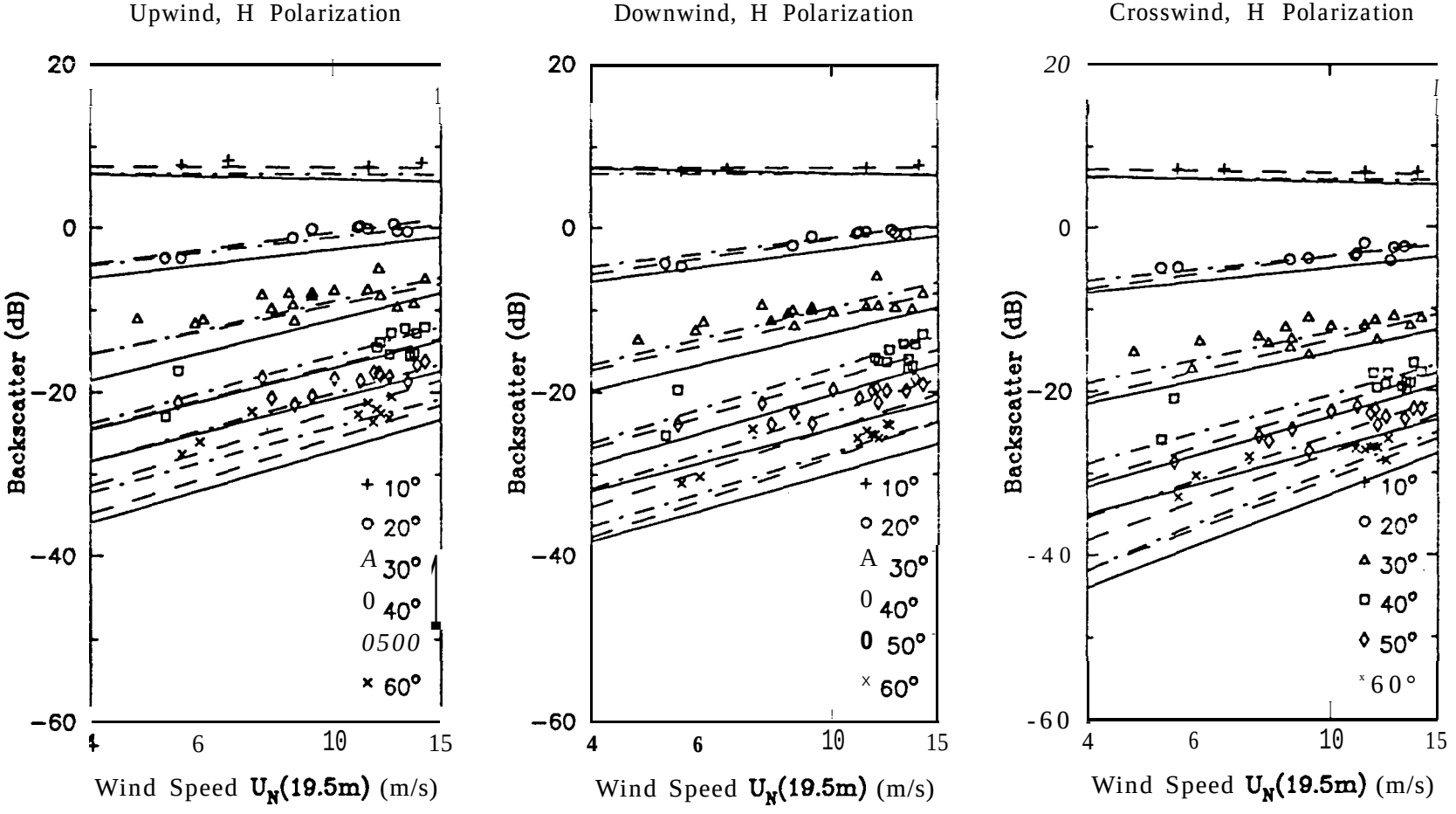

to investigate azimuth modulations in ocean radar backscatter. The modulation was specified in terms of backscatter at upwind, downwind, and crosswind. An algorithm was developed to account for extraneous harmonics introduced by the modulation in incidence angles. Simulations indicated a good performance of the algorithm. NU SCAT/SWADE results are higher than RADSCAT, compared well with SASS- I at small incidence angles, and in good overall agreement with SASS-II.

ACKNOWLEDGMENT

The research described in this paper was carried out by the Jet Propulsion laboratory, California Institute of Technology, under a contract with the National Aeronautics and Space Administration.

REFERENCES

[1] L. C. Schroeder, P. R. Schaffner, J. L. Mitchell, and W. L. Jones, "AAFE RADSCAT 13.9 -GHz measurements and analysis: Wind-speed signature of the ocean," *IEEE J. Oceanic Engineering*, vol. OE-10, no. 4, pp. 346-357, 1985.

[2] W. 1,. Jones, L. C. Schroeder, D. H. Boggs, E. M. Bracalente, R. A. Brown, G. J. Dome, W. J. Pierson, and F. J. Wentz, "The SEASAT-A satellite scatterometer: the geophysical evaluation of remotely sensed wind vector over the ocean," *J. Geophys. Res.*, vol. 87,110. C5, pp. 3297-3317, 1982.

[3] F. M. Naderi, M. 11. Freilich, and D. G. Long, "Spaceborne radar measurement of wind velocity over the ocean - an overview of the NSCAT scatterometer system," *Proceedings of the IEEE*, vol. *79,* no. *6,* pp. *850-866, 1991.*

[4] J. R. Carswell, S. C. Carson, R. E. McIntosh, F. K. Li, G. Neumann, D. J. McLaughlin, J. C. Wilkerson, P. G. Black, and S. V. Nghiem, "Airborne scatterometers: Investigating ocean backscatter under low- and high-wind conditions," Proceedings of *the IEEE*, vol. 82, no.12, p]). 1835-1860, 1994.

[5] S. V. Nghiem, F. K. Li, S. }1. Lou, G. Neumann, R. E. McIntosh, S. C. Carson, J. R. Carswell, E. J. Walsh, M. A. Donelan, W. M. Drennan, "Observations of ocean radar backscatter at Ku and C bands in the presence of large waves during the Surface Wave Dynamics Experiment," *IEEE Trans. Geosci. Remote Sens.,*, vol. *33,* no. *3,* pp. *708-721, 1995.*

[6] S. V. Nghiem, F. K. Li, S. H. Lou, and G. Neumann, "Ocean remote sensing with airborne Ku-Band scatterometer," *Proceedings of OCEANS,* vol. I, pp. 20-24, Victoria, Canada, 1993.

[7] L. C. Schroeder, D. H. Boggs, G. Dome, 1. M. Halberstam, W. L. Jones, W. J. Pierson, and F. J. Wentz, "The relationship between wind vector and normalized radar cross section used to derive SEASAT-A satellite scatterometer winds," *J. Geophys. Res.*, , vol. 87, no. C5, pp. 3318-3336, 1982.

[8] F. J. Wentz, S. Peteherych, and L. A. Thomas, "A model function for ocean radar cross sections at 14.6 GHz," *J. Geophys. Res.*, vol. 89, no. C3, pp. 3689-3704, 1984.